PROCEEDINGS, Thirty-Fourth Workshop on Geothermal Reservoir Engineering
Stanford University, Stanford, California, February 9-11, 2009
SGP-TR-187

A SINGLE-WELL EGS CONFIGURATION USING A THERMOSIPHON

Zhe Wang, Mark W. McClure and Roland N. Horne

Stanford Geothermal Program
Department of Energy Resources Engineering, 367 Panama St.
Stanford University, CA 94305-2220, USA
e-mail: wangzhe@stanford.edu, mcclure@stanford.edu, horne@stanford.edu

ABSTRACT

This paper describes the investigation of a single-well enhanced geothermal system comprised of a downhole thermosiphon and a novel completion design using a downhole heat exchanger. The thermosiphon is a device that takes advantage of the gravity head difference between liquid flowing down the annulus and vapor flowing up the tubing. Without a connection to a large reservoir volume, a downhole heat exchanger will rapidly deplete the heat near the wellbore and cannot generate useful energy output for very long. Therefore to enhance heat extraction, the effectiveness of a second annulus outside the casing was investigated. A working fluid would circulate by natural convection down the outer annulus and upwards through fractures created in the reservoir. This configuration has the advantages that a second injection well is not required, the need for downhole pumping is avoided by the thermosiphon effect, and the fractures carrying fluid through the reservoir makes the system sustainable. A limitation is that reliance on free convection to circulate fluid through an EGS reservoir does not result in large flow rates, which lowers the productivity. We constructed a coupled finite-difference wellbore and reservoir model representing the fluid mechanics, fluid phase behavior and heat transfer. We investigated the energy output of the system and the feasibility of sustainable deployment.

INTRODUCTION

Enhanced Geothermal Systems (EGS) are an attractive prospect for the development of base-load, carbon-free electricity generation. However, achieving EGS electrical generation at a reasonable cost is based upon a number of technological advances to reduce the expense of installation or to increase the rate at which energy can be recovered. This study is investigating an uncommon design for an EGS system, which is a hybrid of a downhole heat exchanger and an EGS fracture network.

The design concept includes a number of novel ideas, including:

1. Use of single well systems in place of multiwell systems, with level-to-level fracturing.
2. Use of downhole heat exchangers in place of surface heat exchangers.
3. Use of gravity head thermosiphons in place of well pumps.
4. Use of downhole circulation of secondary working fluid in place of water.

These four concepts may be expected to have a number of advantages over conventional ideas, as will be described here.

The conventional concept of an EGS includes a region of fractured rock, through which fluid is circulated from one well to another well, Figure 1.

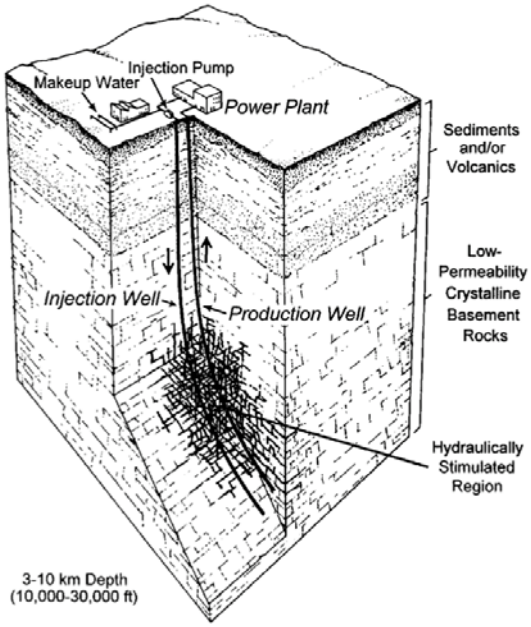

Figure 1: Conventional two-well EGS configuration, from Tester et al. (2006).

An alternative idea is to fracture the formation and then produce and inject in the same well, as in Figure

2. The single well concept removes one of the wells, and circulates fluids from one interval to another within the same well. The fluid may travel down the casing and back up the inner tubing. Variations of this idea have been suggested by a number of authors, including US Patent 4201060 (Outmans, 1980).

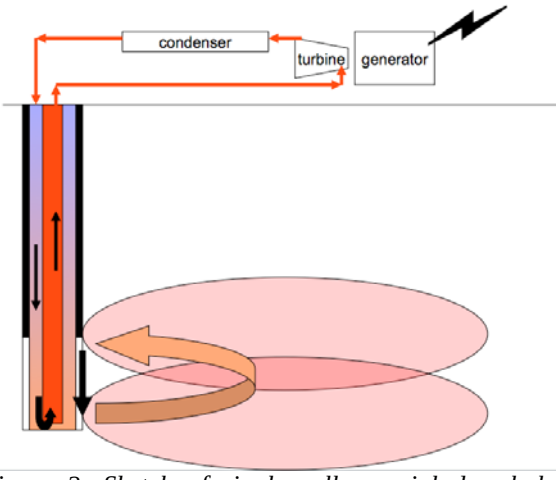

Figure 2: Sketch of single-well, coaxial downhole heat exchanger with fractures.

The advantage of a single-well system is that only one well needs to be drilled (or perhaps an abandoned oil or gas well could be used in which case no wells need to be drilled).

The disadvantage is that the connection of a fracture network to a single well in such a configuration has yet to be demonstrated in a geothermal rock.

Our study includes the concept of a downhole heat exchanger, also shown in Figure 2. Traditional coaxial downhole heat exchangers have been used in direct use applications. The problem with using a device that extracts heat only by conduction is that conduction is unable to bring heat to the wellbore very quickly or for very long, and thus cannot be used for large scale heat extraction (Nalla et al., 2004).

We explored the idea of connecting the heat exchanger to an EGS fracture network, which would bring additional heat to the wellbore. Water would circulate through the reservoir and through an outer annulus, between the outside of the casing and the drilled radius of the wellbore. Circulation through the second annulus and through the reservoir fractures is driven by free convection. The convection brings additional heat to the heat exchanger, and may extend the duration of time that heat can be extracted.

Our idea of enhancing heat flow to the device would be to fracture the formation from two intervals 500 to 1000 m apart, as has been suggested by a number of authors, including US Patent 4201060 (Outmans, 1980). Nalla et al. (2004) analyzed the thermal output of this configuration, albeit with much smaller separation. In such a configuration, as shown in Figure 2, geothermal water would move convectively through the annular space surrounding the heat exchanger, and circulate 500 to 1000 m through the fracture network in the formation. Hence the heat transfer to the heat exchanger is enhanced over simple conduction.

It may also be feasible to use multilateral completions in place of, or as well as, fractures, although that concept is not discussed in this paper.

At least in early adoption, EGS projects are likely to use binary power plants because of their ability to work effectively with lower temperature fluids. Some of the energy losses inherent in geothermal systems using binary power plants are associated with the energy required to pump the geothermal fluid to the surface to pass it through the heat exchangers. An alternative is to circulate the secondary fluid down the well bore, which effectively puts the heat exchanger downhole. An important advantage to this is that there is no longer any need for downhole pumps, which are one of the more problematic components in the operation of a binary geothermal project. Secondary working fluid could be pumped at the surface, where pumps and pump motors operate under more benevolent conditions and are easily accessible for maintenance.

The term thermosiphon (sometimes spelled thermosyphon) is somewhat loosely applied to devices that circulate fluid (and heat) due to variations in buoyancy between fluids of differing temperature and sometimes different phase (liquid and vapor). Among many other applications, the two-phase form of the devices has been used to cool computer processors. It is this two-phase type of thermosiphon that seems most appropriate for geothermal use.

One advantage of thermosiphon in downhole heat exchanger is to remove the need for a downhole pump. Downhole pumps have drawbacks in two ways: firstly, in the harsh downhole environment pumps have relatively short times between repairs; secondly, it is less efficient thermodynamically to use pumps to pressurize the fluid and then use it in heat exchangers on the surface (DiPippo, 2008). Another advantage of the thermosiphon is to make use of the tremendous pressure difference between the outflowing and inflowing fluid to provide a source of hydraulic energy. The thermosiphon effect can be achieved by circulating the secondary working fluid downhole, through the coaxial downhole heat exchanger. The boiling point of the working fluid, (typically isopentane, but other choices are possible),

is lower than that of water, which results in a more prominent thermosiphon effect than would be achieved with water. A second reason to circulate the secondary working fluid is to prevent scaling in the tubing.

The concept of the downhole thermosiphon, depicted in Figure 2, can be described as follows: cold secondary working fluid is injected into the annulus between the tubing and casing, and extracts heat from formation as it flows downward. In the working part of the formation, a second annulus outside the device allows formation fluid to circulate from one fractured interval to the other. There is no contact between the working fluid in the wellbore and in the fluid in the formation. As opposed to only heat conduction, the heat transfer is enhanced by the convective flows in the fracture and in the second annulus. After the downflowing fluid is heated, it will be returned to the surface through the inner tubing. It may be useful to install a choke at the base of the tubing string to depressurize the upflowing fluid to achieve vaporization, which would thus enhance the thermosiphon behavior. Once the thermosiphon is operating, the working fluid would circulate spontaneously in the wellbore, and the pressure difference between upward and downward flows at the surface would be recovered in the binary turbine. At the same time in the fracture system, the fluid in the formation would circulate spontaneously by natural convection. The formation fluid would become denser as it flows down the second annulus, and reheated as it flows upward in the fracture. Thus there would be a second thermosiphon behavior in the EGS fractures, driven by the density difference between the hotter and cooler fluid.

The potential for sustainable power generation from such a downhole heat exchanger concept was studied by coupling two numerical models, one of the wellbore and the other of the reservoir. The wellbore calculation was made with a purpose-built program, and flow in the formation fracture intervals was simulated using a variant of TOUGH2 (Pruess, 1999). In addition to examining well configurations (wellbore geometry, insulation, and depth), we also examined the behavior of the thermosiphon and the influence of different types of fractures. After analyzing the effects of individual factors, we estimated the sustainability of this system by calculating the energy output from it for 30 years, using a hypothetical geological model based on the real EGS field at Soultz (Schindler *et* al., 2008, Tischner *et al.*, 2006).

In preliminary calculations we found that the single-well thermosiphon system produces rather modest power output. The heat production of the system is limited by the amount of heat that can be transferred from the reservoir fracture network to the wellbore. The heat transfer from the reservoir by convection dominates because conduction through the rock to the wellbore is small, especially in the long term. However, the rate of convection is limited by the flow rate through the reservoir. In a conventional two-well EGS design, the density difference exists over the entire length of the wellbores from surface to bottom, and circulation by pumping from the surface is also possible. Therefore a lower rate of heat extraction would be achieved in a system that uses a downhole heat exchanger, unless the circulation rate in the reservoir can be improved.

METHODOLOGY

1. Wellbore Calculations

A numerical wellbore model was built to simulate the heat transfer between coaxial flow in the wellbore and the hot surrounding rock. Heat transfer occurs within the coaxial tubings between upward flow and downward flow, as well as between the wellbore and the surroundings. Mass balance, momentum equation and energy conservation complete the wellbore model (Ouyang and Belanger, 2004).

$$\pi r_w^2 \frac{\partial \rho}{\partial t} = \frac{\partial(\rho q)}{\partial z} \quad (1)$$

$$-\frac{dp}{dz} = -\frac{2\tau_w}{r_w} - \rho g \cos\theta - \frac{\partial(\rho V)}{\partial t} + \frac{\partial(\rho V^2)}{\partial z} \quad (2)$$

in which τ_w is the wall shear stress.

The energy balance can be written as Eq. (3) if we neglect the heat generated by friction:

$$\pi r_w^2 \frac{\partial(\rho u)}{\partial t} = \frac{\partial(\rho q h)}{\partial z} - 2\pi r_w U(T_w - T_r) \quad (3)$$

in which *u* is the specific internal energy and *h* is the specific enthalpy. *U* is the overall heat transfer coefficient, which can be determined by Eq. (4) (Horne, 1980):

$$\frac{1}{U} = \frac{r_o^2}{r_i^2}\frac{1}{h_i} + \frac{r_o}{k_s}\ln\frac{r_o}{r_i} + \frac{1}{h_o} \quad (4)$$

in which r_i and r_o refer to radii of the inner and outer tubings respectively. A sketch of the well configuration is shown in Figure 3. k_s is the thermal conductivity of the pipe and h_i is the convective heat transfer coefficient is given by (Holman, 1968):

$$h_i = \frac{k_f}{r_i} 0.0395(\mathrm{Re})^{0.75} \quad (5)$$

For heat transfer to the surroundings, if we neglect heat convection and the Joule-Thomson effect, the energy balance can be written as Eq. (6):

$$\frac{\partial \rho_f V_{volume} u}{\partial t} = -kA\nabla T \quad (6)$$

In which u is the specific internal energy, k is the (constant) heat conductivity of the formation, A is the interface area.

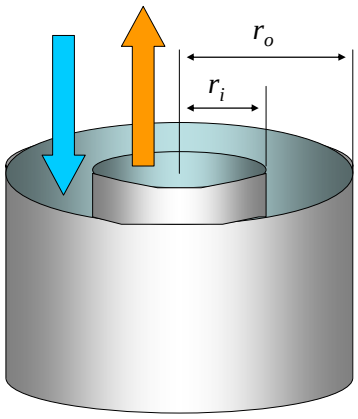

Figure 3: Sketch of the well configuration.

These equations can be solved numerically, by discretizing into finite differences. Cylindrical coordinates were used to describe the radial grid in the formation. To capture the rapid temperature change in the near-wellbore region, we used a logarithmic gridding, as shown in Figure 4. A logarithm spacing was also applied to the time discretization.

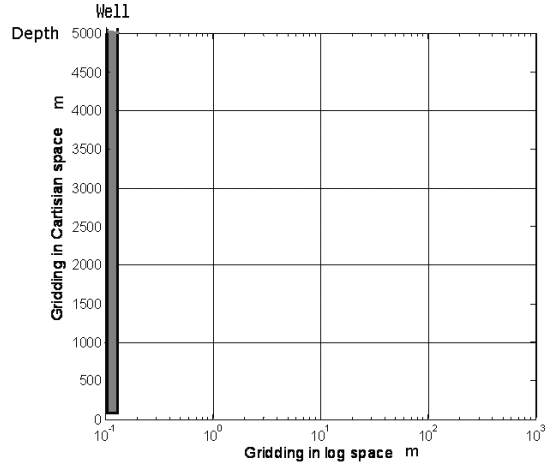

Figure 4: Sketch of gridding in surroundings.

This well model was verified by comparing to the results of the paper by Nalla et al. (2004). In this particular case, the well outlet temperature for 3 years was calculated from a coaxial wellbore heat exchanger which circulates water. The comparison is shown in Figure 5.

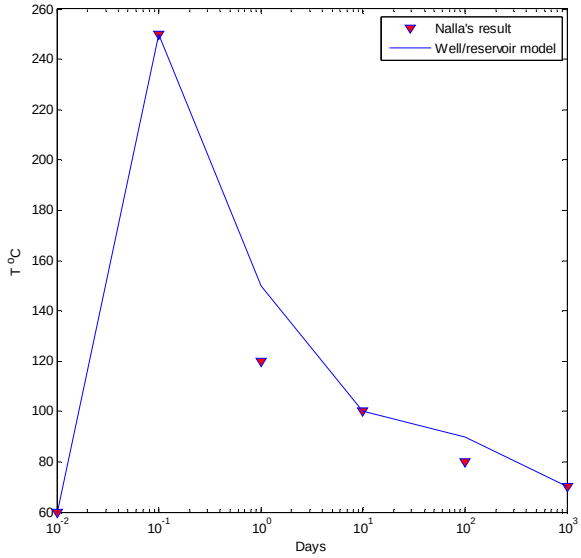

Figure 5: Verification of the well model by comparison to the result of Nalla et al. (2004).

2. Reservoir Fracture Modeling

The reservoir model was constructed to represent a "typical" EGS reservoir. In order to make the model realistic, we used information about the characteristics of the European EGS site at Soultz-sous-Forêts in France. We call our model "Soultz-like" – not intended to be a true representation of Soultz. Soultz is a good site to use an example because it has been the subject of extensive research and characterization. A summary of the reservoir model is given in the body of this paper and additional background is given in Appendix A.

The reservoir model was constructed using AUTOUGH2. AUTOUGH2 was written at the University of Auckland (O'Sullivan, 2000), and is a version of TOUGH2, an integrated finite difference numerical reservoir simulator developed at Lawrence Berkeley National Laboratory (Pruess, 1999). TOUGH2 can simulate nonisothermal, multicomponent, multiphase flow and diffusion.

The "Soultz-like" reservoir model consists of two parallel fracture planes. The two fractures represent two idealized paths through a reservoir. One zone, with higher permeability and smaller volume, is the primary (short circuit) zone. The secondary zone which has lower permeability but greater volume, represents a larger overall flow path throughout the fractured volume. The two path concept matches a conceptual model of the Soultz reservoir that was based on a two well tracer test analyzed in Sanjuan *et al*. (2006). The two fractures are assumed far enough away from each other that they are effectively independent.

The fractures are planar and vertical with the wellbore in the center. Each is 1000 m tall and 1000 m wide. The thickness of the fracture zone is one meter. The short circuit path through the reservoir has a porosity of 1.3% and a permeability of 534 md. The secondary path has a porosity of 2.17% and a permeability of 228 md. The fractures are surrounded by granite basement rock that conducts heat but is not permeable to flow.

Because of symmetry, only one quarter of the total system needs to be gridded. The total flow rate through the system is four times the flow rate through the quarter-system. The grid of each quarter system fracture is 20×20, with blocks 50 m. high and 25 m. wide. The fracture zone of the quarter systems is one half the actual thickness, 0.5 m. Perpendicular to the plane of the fracture, the matrix rock is gridded with 11 blocks in logarithmic spacing from 0.05 m to 50 m. To test the accuracy of the discretization for heat conduction from the rock mass, a one-dimensional heat conduction calculation was performed and compared to the analytical solution. The discrepancy was found to be about 5%.

In the model, the fracture is filled with liquid water. The initial pressure at the top of the reservoir (depth 4 km) is set at 400 bars. The geothermal gradient is 40ºC/km with a surface temperature of 20ºC. Each quarter-system is connected to the well on one side at the top and bottom.

3. Coupling the Two Models

The wellbore model and fracture model each provide boundary conditions for the other, so we used an iterative procedure to equalize the calculated values of flow rate in the second annulus computed from both models. A flow chart is shown in Figure 6. The pressure at the top of the second annulus was set constant at 400 bars, and then starting with an initial guess of the flow rate, the well model provided temperature and pressure values at the bottom of the second annulus. These values were used as input to the fracture model, and then the TOUGH2 model would calculate the fracture outlet temperature and a new flow rate. The process iterated until the flow rate in the annulus and the reservoir converged. The value of flow rate during the iterative process is shown in Figure 7. The process converged after five or six steps if we set the convergence criterion to be 10^{-3} kg/sec.

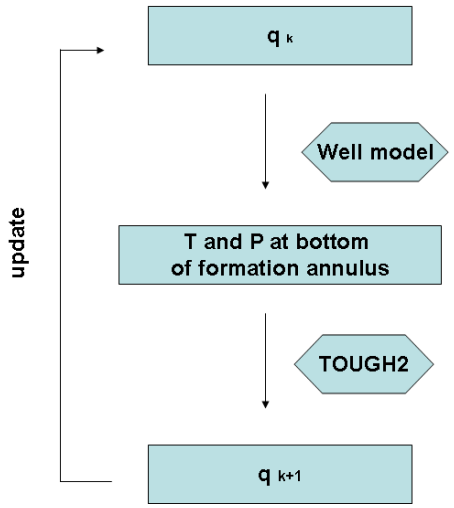

Figure 6: Iterative approach to couple the well model and reservoir model.

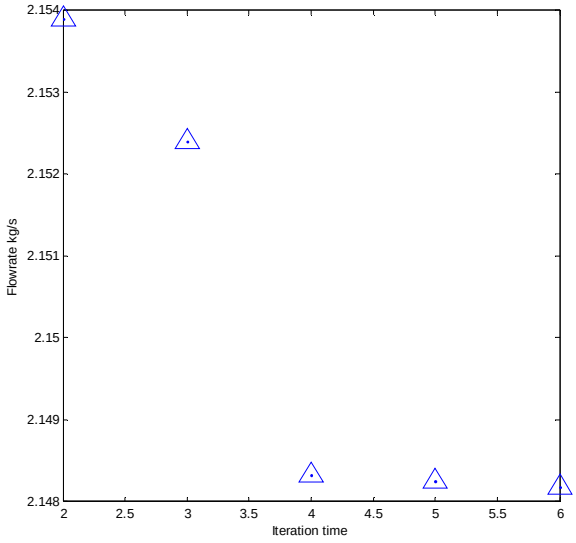

Figure 7: Convergence of the calculated flow rate in the second annulus.

4. Binary Cycle Analysis

A pressure-enthalpy diagram can help to visualize the thermodynamic process in the turbine. The pressure-enthalpy diagram of isopentane is shown in Figure 8. In a traditional binary plant, State 1 defines the inlet condition for the turbine, while State 2 is the turbine outlet. To find the specific enthalpy in State 2, we need to resort to an isentropic process, denoted State 2s, at which point fluid has the same entropy as in State 1, but has pressure and temperature at condenser conditions. When specific enthalpy at State 2s is determined from the fluid thermodynamic properties table by specifying pressure (or temperature) and entropy, the specific enthalpy at State 2 can be calculated. The overall ideal work efficiency can be determined from Eq. (7):

$$\eta = \frac{h_1 - h_2}{h_1 - h_{2s}} \quad (7)$$

The specific work available in the turbine (kJ/kg) is calculated by Eq (8):

$$w_t = h_1 - h_2 \quad (8)$$

The electrical power generated can be calculated by the product of mass flowrate and turbine specific work.

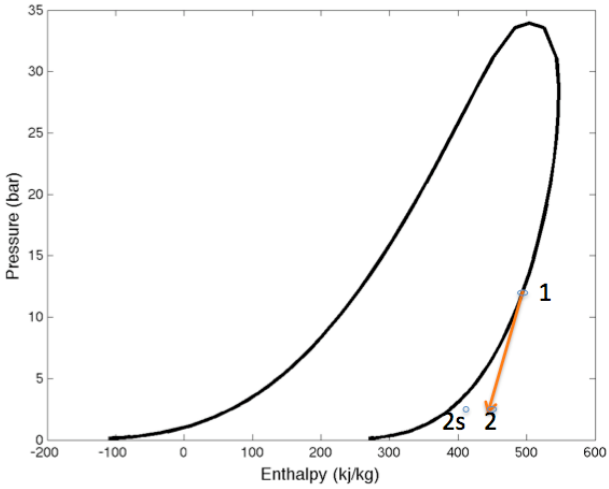

Figure 8: Pressure-enthalpy diagram of isopentane.

Table 1: Common parameters in bae configuration.

Thermal environment	
Working fluid	Isopentane (i-C_5H_{12})
Mass flowrate	2 kg/s
Surface temperature	20 °C
Geothermal gradient	40 °C/km
Formation volume heat capacity	900 kJ/m^3 °C
Formation thermal conductivity	2 W/m °C
Formation density	2000 kg/m^3
Formation thermal diffusivity	10^{-6} m^2/s
Well geometry	
Casing diameter	340 mm
Tubing diameter	65 mm
Insulation material conductivity	0.05 W/m °C
Insulation thickness	5 mm
Binary cycle specification	
Condenser temperature	320 K
Turbine isentropic efficiency	85%

SENSITIVITY STUDY

Effects of several parameters were examined in the sensitivity study. The basic configuration shared by the examples shown in this paper is summarized in Table 1. All the values were chosen to make the model realistic, e.g. the geothermal gradient and thermal conductivity of the formation are set to be typical in value.

As for electricity power generation, we assumed a constant condenser condition at 320 K, which corresponded to a pressure of 1.866 bar, which is also the condition for the working fluid injected back into wellbore. Another assumption here is the isentropic turbine efficiency of 85%. The well is cased all the way down to the bottom, and the inner tubing is insulated.

1. Insulation of inner tubing

As shown in previous studies on coaxial downhole heat exchangers, e.g. Horne (1980), insulation of the tubing is a crucial factor for effective heat extraction from the formation. A comparison of the temperature profile with and without inner tubing insulation is shown in Figure 9. It is clear that the well outlet temperature will approach the inlet temperature if there is no insulation of the inner tubing. Conversely, the outlet temperature is much higher with the inner tubing insulated. Hence, more energy is extracted from the formation with an insulated tubing. A comparison of thermal power output over 30 years is shown in Figure 10.

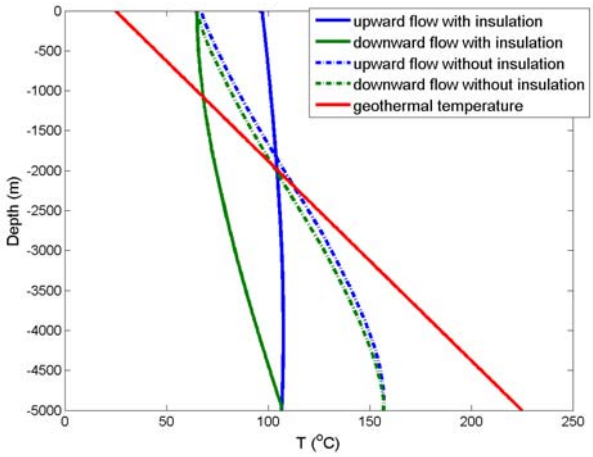

Figure 9: Temperature profiles.

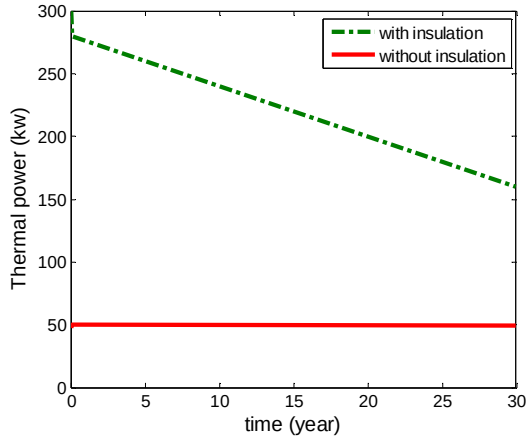

Figure 10: Thermal power output from tubing with insulation and without insulation.

2. Well geometry

The effects of the outer wellbore radius would be twofold: the bigger the well, the more energy it would extract from the formation; however a bigger well would deplete the formation more quickly. Figure 11 shows the thermal power output using different casing diameters after operation for one month. We can see that the power increases as the casing becomes larger, which is consistent with our expectation. For a sustainability issue, as shown in Figure 12 the bigger well can still generate larger power, although it has faster rate of decline.

The effect of tubing size was also studied, as shown in Figure 13; a small tube is preferable from a thermal output point of view, although it must be remembered that reducing the size would increase the pressure drop and would ultimately prevent flow.

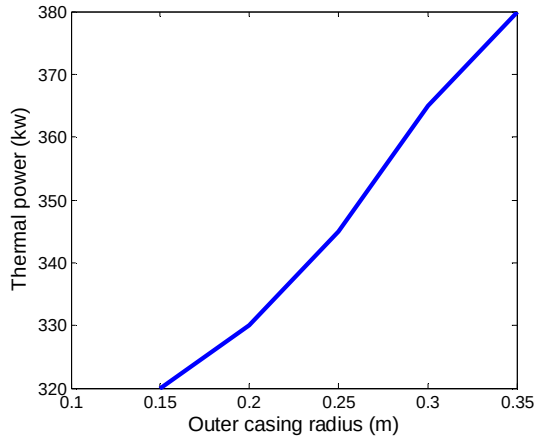

Figure 11: Thermal power output after 1 month operation, as a function of outer casing radius.

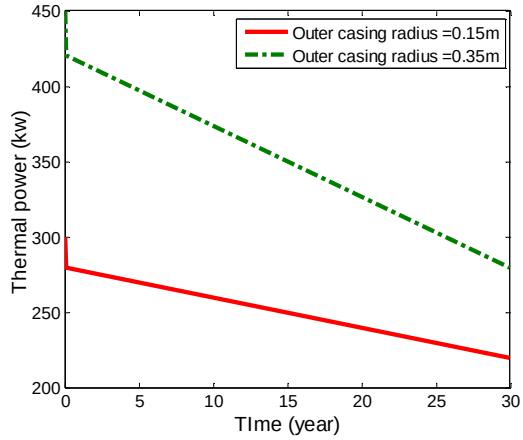

Figure 12: Thermal power generation histories for different outer casing radius.

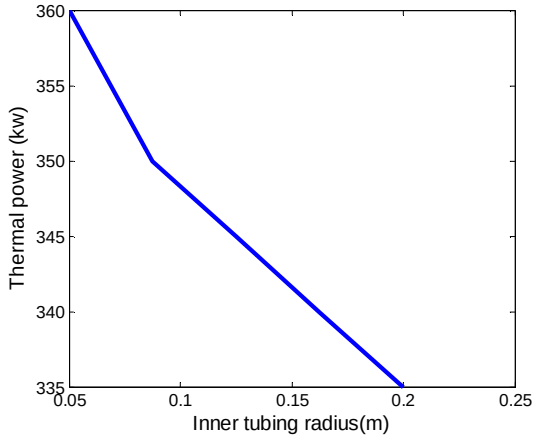

Figure 13 Thermal power generation after 1 month over different tubing radius

3. Flow rate

The electrical power output depends on the mass flow rate of working fluid and the specific enthalpy at the inlet of turbine. So we can not say that a higher flow rate guarantees greater energy output, because for slower flow there would be a larger specific enthalpy to input into the turbine. This results from a longer residence time in the wellbore thereby extracting more energy from the formation. As shown in Figure 14, a higher flow rate would decrease the well outlet temperature and the ideal work has an optimum value at a specific flow rate.

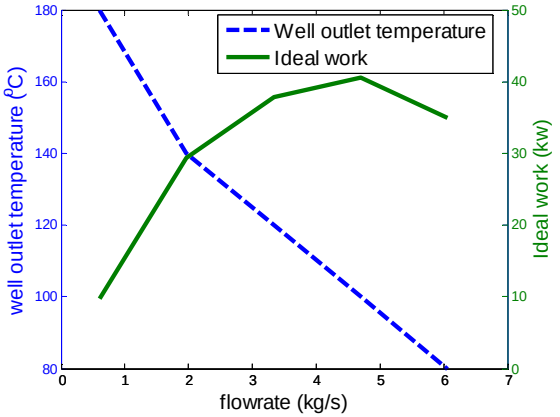

Figure 14: Well outlet temperatures and ideal work for different flow rates after 1 month operation.

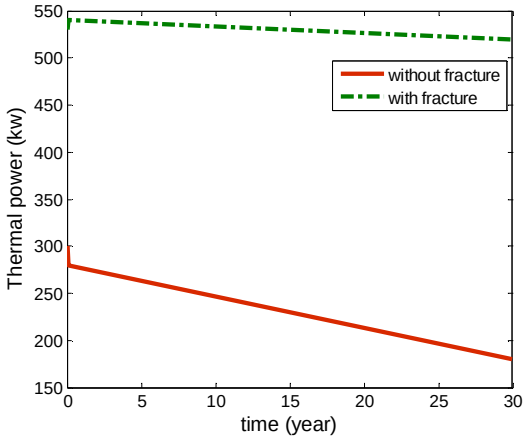

Figure 15: Thermal power output with fracture and without fracture.

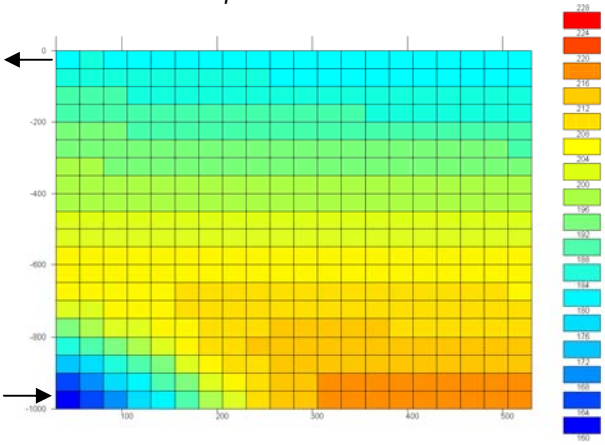

Figure 16: Temperature distribution in the primary connection fracture after 30 years. This image was made with Mulgraph.

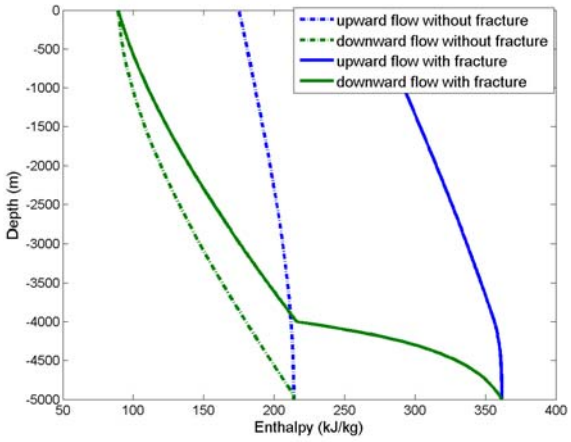

Figure 17: Specific enthalpy in wellbore after production for 1 month

4. Fracture connection

The connection of the heat exchanger to a reservoir fracture brings additional heat to the wellbore and increases the energy that can be produced from the system. The connection increases the length of time the system can produce energy, from a far greater volume of rock.

Figure 15 shows that with flow in the fracture the extracted thermal energy decreases very little even after 30 years. The reason is that the rate of heat extraction is sufficiently small that thermal breakthrough in the fracture does not occur in this case.

Figure 16 shows the temperature distribution in the primary connection fracture after 30 years. Because of symmetry, only half of the total fracture is shown. The well is located at the left of the figure. Total flow rate was approximately constant around 2.5 kg/sec. About 70% of the total flow went through the primary connection fracture, and 30% through the secondary. This image was made using Mulgraph (O'Sullivan and Bullivant, 1995).

Figure 17 shows the advantage that the fracture brings in increasing the enthalpy of the fluid circulating in the downhole heat exchanger.

The flow rate in the fracture (and second annulus) is relatively low because the driving force is not large. The flow is driven by natural convection because temperature in the second annulus, where heat is being removed, is lower than temperature in the

reservoir. The density difference caused by the temperature variation is roughly 100 kg/m^3. Over a distance of one kilometer, that comes out to about 10 bar of driving force. For comparison, the Soultz reservoir managed 12 kg/sec of flow with a pressure difference of 66 bar (see Appendix A).

5. Gravity thermosiphon

One reason to circulate secondary working fluid through the wellbore is that it is more volatile as temperature increases. By placing a choke at the bottom of the well, we may achieve a phase change as fluid rises in the inner tubing. The density difference caused by phase change becomes a force to support the flow and the well outlet pressure is higher than the inlet pressure. This pressure difference can force the fluid to circulate spontaneously, and can provide hydraulic energy to the turbine for electrical generation. Figures 18, 19 and 20 show vapor fraction, pressure and temperature distributions in the wellbore after operation for 1 month, showing the phase change in the upward flow when the downhole choke is used. To illustrate the thermosiphon effect, the example shown used a hotter reservoir with geothermal gradient to be 60^{o}C/km, all other specifications are as in Table 1. Figure 21 shows the enthalpy in the two cases, showing that the choke does not change the enthalpy distribution in the wellbore. Figure 22, shows the operating cycle on a pressure-enthalpy diagram. Starting from the outlet of the condenser, State 1, fluid is injected into the outer casing; and pressure and specific enthalpy increase as it flows downwards, until it reaches the bottom of casing, at State 2. At the bottom of the tubing, fluid passes through the choke and starts flowing upwards, at State 3. As the fluid loses pressure and enthalpy, it will go through a two-phase region and finally become superheated at the well outlet. This superheated vapor enters the turbine undergoing a process shown earlier in Figure 8. The dry gas exiting the turbine is passed into the condenser, and the loop is closed.

In the thermosiphon case, the cycle follows the path 1-2-3-4, whereas for the case without the thermosiphon it follows 1-2-3'-4'. Without the thermosiphon, the fluid would arrive at the turbine inlet in a liquid state; with the thermosiphon it arrives in a vapor state.

A calculation of the long term electrical power generation in this example is shown in Figure 23.

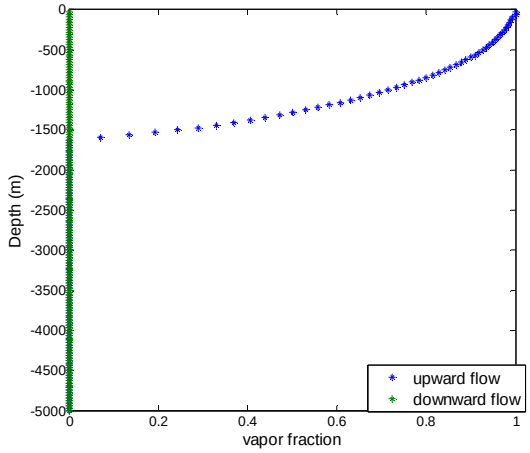

Figure 18: Vapor fraction in the wellbore, with a downhole choke.

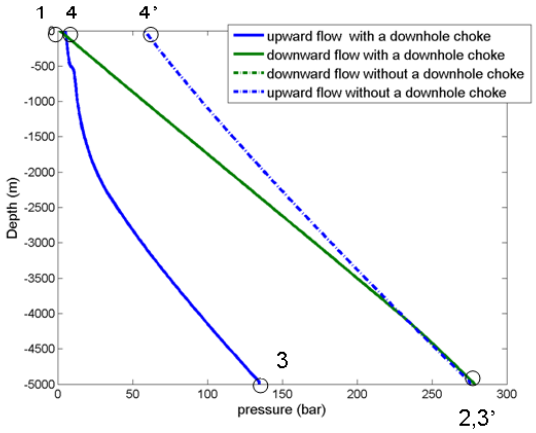

Figure 19: Pressures in the wellbore, with and without a downhole choke.

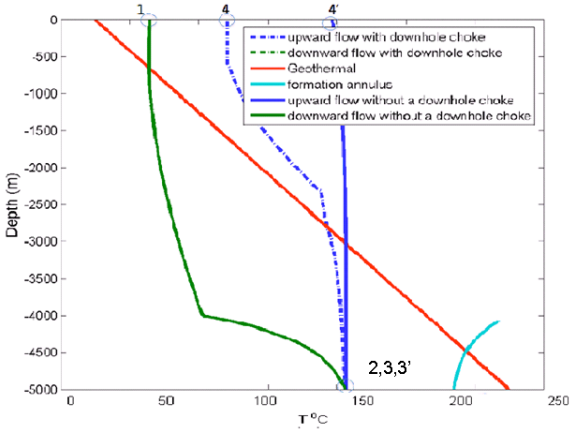

Figure 20: Temperatures in the wellbore, with and without a downhole choke.

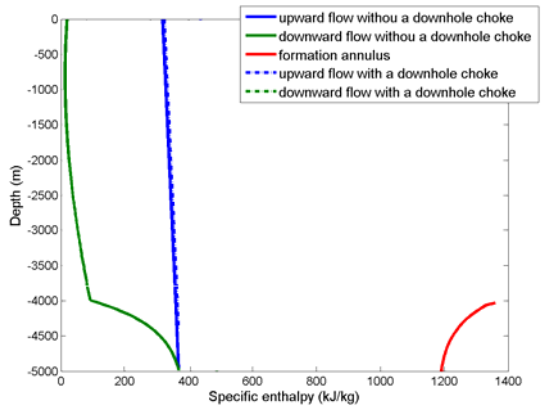

Figure 21: Enthalpy in the wellbore and formation annulus, with and without a downhole choke

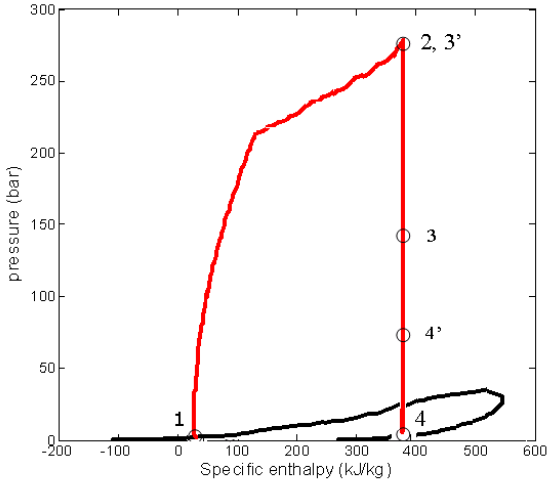

Figure 22: Pressure-enthalpy diagram of the complete cycle. 1-2-3-4 for thermosiphon case; 1-2-3'-4' without the thermosiphon.

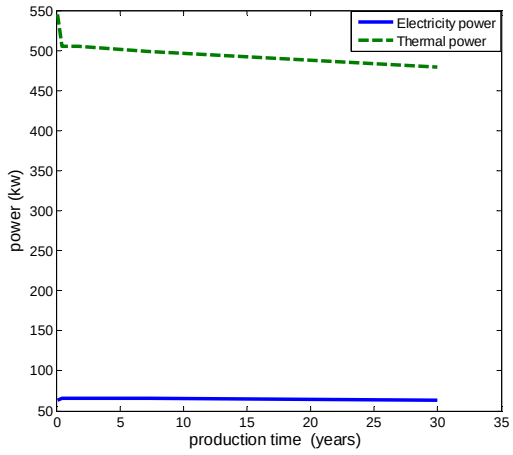

Figure 23: Thermal and electrical power generation histories for 30 years.

CONCLUSIONS

We studied the power generation capacity of a novel downhole concept with the several differences over traditional EGS designs. These differences are:

1. Use of single well systems in place of multiwell systems, with level-to-level fracturing.
2. Use of a downhole heat exchanger in place of surface heat exchangers.
3. Use of a gravity head two-phase thermosiphon in place of well pumps.
4. Use of downhole circulation of secondary working fluid in place of water.

The effects of these several factors have been examined, summarized as follows:

1. Insulation of the inner tubing is critical to transporting sufficient heat to the surface.
2. Without the benefit of fracture circulation, which introduces convective heat flow, the system would be of modest power generating capacity and would decline quickly.
3. The thermosiphon can be beneficial in providing a more advantageous energy cycle.

FUTURE WORK

Topics of further work on the downhole heat exchanger and thermosiphon will include using different working fluids and reversing the direction of flow in the heat exchanger.

Up to this point we have found that the downhole heat exchanger is not very advantageous because it limits the flow rate through the EGS reservoir, which is a critical parameter for heat extraction. Methods to enhance the reservoir flow are under investigation.

ACKNOWLEDGEMENT

This research has been funded by a grant from Google.Org. We are grateful for their support.

REFERENCES

DiPippo, R.D.: *"Geothermal Power Plants,"* Second Edition, Elsevier, Oxford, 2008.

Genter, A., Traineau, H., Ledésert, B., Bourgine, B., and Gentier, S.: "Over 10 Years of Geological Investigations within the HDR Soultz Project, France," Proceedings World Geothermal Congress, 2000.

Holman, J.P.: "*Heat Transfer,*" Second Edition, McGraw-Hill, New York, 1968.

Horne, R.N.: "Design Considerations of a Downhole Coaxial Geothermal Heat Exchanger," Geothermal Resources Council *Transactions*, **4**, 569, 1980.

Nalla, G., Shook, G.M., Mines, G.L., and Bloomfield, K.: "Parametric Sensitivity Study of Operating and Design Variables in Wellbore Heat Exchangers," Workshop on Geothermal Reservoir Engineering, Stanford University, 2004.

O'Sullivan, M.J., Bullivant, D.P.: "A Graphical Interface to the TOUGH2 Family of Simulators," Proceedings of the 1995 TOUGH Users Workshop, http://esd.lbl.gov/TOUGHPLUS/proceedings/1995/OSullivanBullivant.pdf

O'Sullivan, M.J.: "AUTOUGH2 Notes", Department of Engineering Science, University of Auckland, p.18. (2000).

Outmans, H.D.: "Geothermal Power Plant," US Patent 4201060, 1980.

Ouyang, L.B., and Belanger, D.: "Flow Profiling via Distributed Temperature Sensor System-Expectation and Reality," SPE 90541, SPE Annual Technical Conference and Exhibition, 26-29 September 2004, Houston, TX (also *SPE Production & Operations*, **21**(2), (May 2006), 269-281.)

Date May 2006

Pruess, K., Oldenburg, C., and Moridis, G. *TOUGH2 User's Guide, Version 2.0," Ernest Orlando Lawrence Berkeley National Laboratory, 1999.*

Ramey, H.J., Jr.: "Wellbore Heat Transmission," *J. Pet. Tech.* (April 1962), 427-435, *Trans.*, AIME, **225**.

Reynolds, W.C.: "*Thermodynamic Properties in SI: Graphs, Tables and Computational Equations for 40 Substances,"* Dept. of Mechanical Engineering, Stanford University, Stanford, CA, 1797.

Sanjuan, B., Pinault, J., Rose, P., Gérard, A., Brach, M, Braibant, G., Crouzet, C., Foucher, J., Gautier, A., Touzelet, S. (2006): "Tracer testing of the geothermal heat exchanger at Soultz-sous-Forêts (France) between 2000 and 2005," *Geothermics*, **35**, 622-653.

Sausse, J., Dezayes, C., Genter, A., and Bisset, A.: "Characterization of Fracture Connectivity and Fluid Flow Pathways Derived from Geological Interpretation and 3D Modelling of the Deep Seated EGS Reservoir of Soutlz (France)," Workshop on Geothermal Reservoir Engineering, Stanford University, 2008.

Sausse, J.: "Hydromechanical properties and alteration of natural fracture surfaces in the Soultz granite (Bas-Rhin, France)," *Tectonophysics*, **348**, 169-185.

Schindler, M., Nami, P., Schellschmidt, R., Teza, D., Tischner, T.: "Summary of Hydraulic Stimulation Operations in the 5 km Deep Crystalline HDR/EGS Reservoir at Soultz-Sous-Forêts," Workshop on Geothermal Reservoir Engineering, Stanford University, 2008.

Tester, J.W. (ed.): "*The Future of Geothermal Energy Impact of Enhanced Geothermal Systems (EGS) on the United States in 21st Century,"* MIT Report, 2007.

Tischner, T., Pfender, M. and Teza, D.: "Hot Dry Rock Projekt Soultz: Erste Phase der Erstellung einer wissenschaftlichen Pilotanlage," Bundesministerium für Umwelt, Naturschutz und Reaktorsicherheit, 2006.

APPENDIX A:

It would valuable to provide some background on the European EGS site at Soultz-sous-Forêts in the Upper Rhine Graben in North-East France. Information about the Soultz reservoir was used as a source to help design a "reasonable" model of an EGS reservoir for use in this study. We called our model "Soultz-like" – not intended to be a true representation of Soultz.

The wells at Soultz were drilled into the fractured crystalline basement rock, which is covered by 1400m of Cenozoic and Mesozoic sediments. In the 1990s, wells were drilled to a depth of 3700 m and a shallow EGS reservoir was formed (Genter *et al*., 2000). From 2000 onward three wells were deepened to a depth of 5000 m and stimulated to form a reservoir. The wells are approximately 600 m. apart, and connect to the formation through 500 m of open borehole. The initial permeability of the formation was very low, but a series of hydraulic stimulations were carried out to enhance the natural permeability. Hydraulic stimulation caused shearing on preexisting fractures which were near vertical and optimally oriented with respect to the direction of maximum horizontal stress. The granite is pervasively fractured, but only a small number of fractures intersecting the wellbore were significantly enhanced. The fractures retain their productivity after the stimulation is finished. The productivity enhancement of the formation has been estimated to be at least 20 times the initial permeability. Microseismic monitoring was used to track the growth of the fractured network, and the

microseismic clouds caused by the stimulations occupied a region roughly 300-700 m wide, 500-1000 m tall, and 2000-2500 m long (Schindler *et* al., Tischner *et al.*, 2006).

Our conceptual reservoir model was based on the Sanjuan *et al*. (2006) analysis of tracer tests carried out between the Soultz wells GPK2 and GPK3 between 2000 and 2005. The third deep Soultz well, GPK4, was not considered in this study. Two general fluid pathways between GPK2 and GPK3 are believed to exist. The primary fluid pathway is believed to correspond to a major fracture zone that intersects GPK2 and GPK3 (Sausse *et al.*, 2008) and which flow logs show receives around 70% of flow in GPK3. The remaining flow can be considered to make up a secondary, slower connection between the wells (Tischner *et al*., 2006).

During a 2005 tracer test, 150 kg of fluorescein was injected over 24 hours followed by five months of circulation from GPK3 to GPK2 and GPK4. GPK3 injected at 15 kg/sec., GPK2 produced at 12 kg/sec. and GPK4 produced at 3 kg/sec. The downhole pressure differential between GPK3 and GPK4 was estimated at 66 bar (Tischner *et al*., 2006). Tracer was first detected at GPK2 four days after the injection and peaked from 11-17 days. Sanjuan *et al*. (2006) interpreted the results considering advective and dispersive transport. Their results are summarized in Table 2. They conceptualized the reservoir as consisting of two zones, a short circuit zone and a larger, general reservoir zone. They suggested that native brine water is encroaching into the Soultz reservoir but we did not include brine water encroachment in our model.

Table 2: Soultz estimated fracture properties (from Sanjuan et al., 2006).

Connection	Mean Velocity	Swept Volume
Primary	1-1.2 m/hr	3900 m^3
Secondary	0.3 m/hr	6500 m^3

We modeled both flow zones as isolated vertical fractures. The fractures roughly match the dimensions of Soultz, 500 m tall and 600 m separation between wells. Once the reservoir parameters were determined, the dimensions of the fractures were changed to 1000 m tall and 1000 m wide.

The primary (short circuit) connection was modeled as a 1 m wide zone with a porosity = (3900 m^3 swept volume)/(600 m long*500 m tall*1 m thick) = 1.3%.

The secondary connection represents the part of the fractured reservoir between GPK2 and GPK3 that does not lie in the single primary fracture zone. The cross sectional area of this zone is estimated as (6500 m^3 swept volume)/(500 m tall*600 m long)= 2.17 cm. The fractures in Soultz have been measured to have a mean aperture from 0.5 to 1 mm (Sausse, 2002). That implies that there are roughly 20-40 fractures between the two wells. The spatial distribution of these fractures is not known. The two end members would be: (1) having the entire fractured volume clustered into one zone and (2) having the fractures evenly spaced throughout the reservoir. We chose the worst case scenario. The entire secondary connection is lumped into a single fractured zone, which is one meter wide. The porosity of the zone is therefore 2.17%.

The fracture permeabilities could have been calculated directly from the two well flow test assuming one-dimensional flow and Darcy's law. However the assumption of one-dimensional flow might be unrealistic because it implies that the water enters the fracture uniformly along the length of the well. In reality wells connect to fracture zones through a single point of intersection.

To determine permeability, a model was constructed in TOUGH2 in the general shape of Soultz, 500 m tall 600 m long. The two-well flow test was recreated with 66 bar of pressure difference between the wells. The reservoir was a constant 200ºC and around 400 bar of pressure. The wells connected to the fractures at a single point in the middle of the fracture zone. The permeability of the fractures was altered until the flow rates were 8.4 kg/sec through the primary connection and 3.6 kg/sec through the second. The final permeabilities were 534 md and 228 md for the primary and secondary zones, respectively. The one-dimensional flow assumption yielded permeabilities of 240 md and 103 md.